RESEARCH ARTICLE

Blood vessel anastomosis is spatially regulated by Flt1 during angiogenesis

Jessica E. Nesmith[1], John C. Chappell[2,3,*], Julia G. Cluceru[2,‡] and Victoria L. Bautch[1,2,3,4,§]

ABSTRACT

Blood vessel formation is essential for vertebrate development and is primarily achieved by angiogenesis – endothelial cell sprouting from pre-existing vessels. Vessel networks expand when sprouts form new connections, a process whose regulation is poorly understood. Here, we show that vessel anastomosis is spatially regulated by Flt1 (VEGFR1), a VEGFA receptor that acts as a decoy receptor. *In vivo*, expanding vessel networks favor interactions with *Flt1* mutant mouse endothelial cells. Live imaging in human endothelial cells *in vitro* revealed that stable connections are preceded by transient contacts from extending sprouts, suggesting sampling of potential target sites, and lowered Flt1 levels reduced transient contacts and increased VEGFA signaling. Endothelial cells at target sites with reduced Flt1 and/or elevated protrusive activity were more likely to form stable connections with incoming sprouts. Target cells with reduced membrane-localized Flt1 (mFlt1), but not soluble Flt1, recapitulated the bias towards stable connections, suggesting that relative mFlt1 expression spatially influences the selection of stable connections. Thus, sprout anastomosis parameters are regulated by VEGFA signaling, and stable connections are spatially regulated by endothelial cell-intrinsic modulation of mFlt1, suggesting new ways to manipulate vessel network formation.

KEY WORDS: Angiogenesis, Endothelial cells, Anastomosis, VEGF-A, VEGFR1, Flt1 isoforms

INTRODUCTION

Blood vessel formation is an essential, conserved process in vertebrates that provides oxygen and nutrients to tissues and organs (Carmeliet, 2005; Adams and Alitalo, 2007; Chappell and Bautch, 2010). Aberrant angiogenesis is associated with disease; for example, tumor angiogenesis is one of the hallmarks of cancer (Hanahan and Weinberg, 2011). Blood vessel development during embryogenesis is a multistep process that begins with primitive vessel formation from endothelial progenitor cells via vasculogenesis (Risau and Flamme, 1995; Drake and Fleming, 2000; Xu and Cleaver, 2011), and the subsequent formation of branched vessel networks by sprouting angiogenesis. Sprouting angiogenesis is initiated by endothelial cells that proliferate, extend processes, migrate into extravascular space, and finally connect, or anastomose, with another vessel (Betz et al., 2016; Blanco and Gerhardt, 2013; Larrivée et al., 2009).

Vascular endothelial growth factor A (VEGF) is one of several developmental signaling pathways required for sprouting angiogenesis (Shibuya, 2013; Simons et al., 2016). VEGF binds to the endothelial cell-expressed receptor tyrosine kinases Flk1 (VEGFR2, Kdr) and Flt1 (VEGFR1). VEGF-bound Flk1 triggers a signaling cascade that promotes endothelial cell proliferation, chemotaxis and cell survival, thereby initiating and sustaining sprouting angiogenesis (Khurana et al., 2005; Koch et al., 2011). Flt1 is alternatively spliced to generate two isoforms: a membrane-localized tyrosine kinase receptor (mFlt1) and a soluble isoform lacking the transmembrane and tyrosine kinase domains (sFlt1) (Kendall and Thomas, 1993). Both isoforms of Flt1 have a 10-fold higher binding affinity for VEGFA ligand than Flk1, and complete genetic deletion is embryonic lethal in mice (Kendall and Thomas, 1993; Fong et al., 1995). Nonetheless, sFlt1 cannot independently signal, and mFlt1 has weak kinase activity that is not required for developmental angiogenesis (Ito et al., 1998; Hiratsuka et al., 1998). Thus, Flt1 functions as an endothelial cell-intrinsic decoy receptor or ligand sink to negatively modulate VEGF signaling amplitude during angiogenesis.

Stages of sprouting angiogenesis include sprout initiation, extension, anastomosis, and lumenization (Chappell et al., 2011; Geudens and Gerhardt, 2011). Sprout initiation, extension and lumen formation are relatively well understood processes, whereas anastomosis is less so. Recent zebrafish studies revealed a role for endothelial cell filopodia in vessel anastomosis, and found that adherens junction-mediated cell rearrangements subsequent to connection promote lumen formation (Lenard et al., 2013; Phng et al., 2013). However, it is unknown whether the site or timing of sprout anastomosis is regulated.

We recently showed that Flt1 positively affects the stability of new conduits, suggesting that Flt1 might regulate aspects of anastomosis that affect stability (Chappell et al., 2016). Here, we show that extending sprouts form transient contacts before establishing stable connections. Flt1 regulates the frequency of transient contacts and the probability of a target site being used for a permanent connection, and this spatial selectivity requires mFlt1. These results indicate that blood vessel anastomosis is temporally and spatially regulated by endothelial cell-intrinsic signaling.

RESULTS

Flt1 influences retinal vessel interactions

Global or vascular-selective deletion of *Flt1* in mouse postnatal retinal vessels increases overall sprouting (Chappell et al., 2009; Ho et al., 2012; J.C.C. and V.L.B., unpublished). To examine the role of negative modulation of VEGFA signaling in sprout anastomosis, we

[1]Curriculum in Genetics and Molecular Biology, The University of North Carolina at Chapel Hill, Chapel Hill, NC 27599, USA. [2]Department of Biology, The University of North Carolina at Chapel Hill, Chapel Hill, NC 27599, USA. [3]Lineberger Comprehensive Cancer Center, The University of North Carolina at Chapel Hill, Chapel Hill, NC 27599, USA. [4]McAllister Heart Institute, The University of North Carolina at Chapel Hill, Chapel Hill, NC 27599, USA.
*Present address: Center for Heart and Regenerative Medicine, Virginia Tech Carilion Research Institute, Roanoke, VA 24014, USA. ‡Present address: Department of Pharmaceutical Sciences and Pharmacogenomics, University of California San Francisco, San Francisco, CA 94158, USA.

§Author for correspondence (bautch@med.unc.edu)

V.L.B., 0000-0003-2135-5153

used low-dose tamoxifen treatment to induce mosaic excision of *Flt1* in retinal vessels. We monitored individual endothelial cells lacking *Flt1* function using an excision reporter to visualize Cre recombinase activity via tdTomato expression (Fig. 1).

Sprouts were defined as previously described (Chappell et al., 2009), and interactions between sprouts and vessels at the vascular front were identified in mouse retinas at postnatal day (P) 5 (Fig. 1Ai-iii). The interacting endothelial cells were classified based on cytoplasmic reporter expression or lack thereof in the endothelial cell from which filopodia extended (Fig. 1B,C). Wild-type (WT) sprouts were linked to $Flt1^{-/-}$ endothelial cells significantly more often than to WT cells, and this bias differed significantly from the frequency of $Flt1^{-/-}$ endothelial cells in retinal vessels (Fig. 1D). Because loss of *Flt1* is reported to bias endothelial cells to the tips of vascular sprouts (Jakobsson et al., 2010), we also measured mosaicism at the retinal vascular front and found an insignificant bias that did not account for the frequency of WT sprouts that showed interactions with $Flt1^{-/-}$ endothelial cells (Fig. 1D). These

data suggest that reduced Flt1 levels in endothelial cells promote sprout interactions that are likely to lead to new branches. However, further analysis of sprout anastomosis in mouse retinas was hampered by our inability to follow this dynamic process over extended time periods and determine what precedes and follows the observed static interactions. Moreover, most retinal interactions are at the front and consist of two sprouts intersecting, which does not allow for analysis of target site selectivity.

Transient contacts precede stable blood vessel connections

To better understand the dynamics of blood vessel anastomosis, we turned to primary human umbilical vein endothelial cells (HUVECs) in a 3D sprouting angiogenesis assay to model mammalian angiogenesis and anastomosis *in vitro* (Nakatsu and Hughes, 2008). HUVECs coated onto beads and placed in a fibrin matrix form lumenized sprouts that often connect with targets over 3-7 days. LifeAct-expressing HUVECs were imaged from days (d) 3-5 of sprouting, allowing for visualization of F-actin in live cells and dynamic assessment of endothelial cell behaviors preceding and during anastomosis (Fig. 2A, Movie 1). We were surprised to see two distinct forms of interaction between extending sprouts and potential targets. We scored cytoplasmic extensions from the sprout that exhibited brief, limited interactions (present for only one 10 min frame) with potential targets, that we termed transient contacts (Fig. 2Ai-iv, Fig. S1A,B). Transient contacts were observed with LifeAct fluorescence and with differential interference contrast (DIC) optics (Fig. 2Ai-iv). We also documented interactions of longer duration, termed stable connections, that persisted for at least 30 min and were often coincident with a widened sprout front and/or lumen formation (Fig. 2Av-viii). Transient contacts occurred on average four times prior to a sprout forming a stable connection (Fig. 2B). These transient contacts occurred throughout the lifetime of the sprout and at varying distances from the eventual connection site (Fig. 2C,D).

To further characterize the transient contacts that precede stable sprout connections, we quantified the LifeAct fluorescence intensity at transient contact locations prior to, during, and subsequent to the transient contact (Fig. 2E,F). Fluorescence intensity in the contact area was increased at the contact site compared with either side (Fig. 2E) and was higher at the contact site during contact than at either pre-contact or post-contact times (Fig. 2F), confirming the transient nature of these interactions. Taken together, these results indicate that endothelial cell cytoplasmic extensions transiently 'sample' potential target areas before forming a sustained connection.

Flt1 regulates the number of transient contacts

Given the observed effects of *Flt1* loss on sprout anastomosis *in vivo*, we hypothesized that blood vessel anastomosis is a regulated rather than a stochastic process, and we further posited that VEGFA signaling regulates aspects of anastomosis. We manipulated VEGFA signaling in HUVECs by reducing levels of the negative modulator Flt1. We generated and validated a lentivirus shRNA targeted against both isoforms of *FLT1* (Fig. S2A,B) and showed a high infection efficiency by flow cytometry (Fig. S2C). We used the sprouting angiogenesis assay and analysis of two static endpoints to verify effects of *FLT1* knockdown (KD) (Fig. S2D,E). The number of HUVEC sprouts that emanate from each bead was used to assess overall efficiency of the assay, and this parameter was unaffected by *FLT1* KD (Fig. S2F). By contrast, branch point numbers, a static outcome of numerous endothelial cell behaviors that include, but are not limited to, anastomosis, were significantly increased by *FLT1* KD (Fig. S2G), supporting the predicted effects
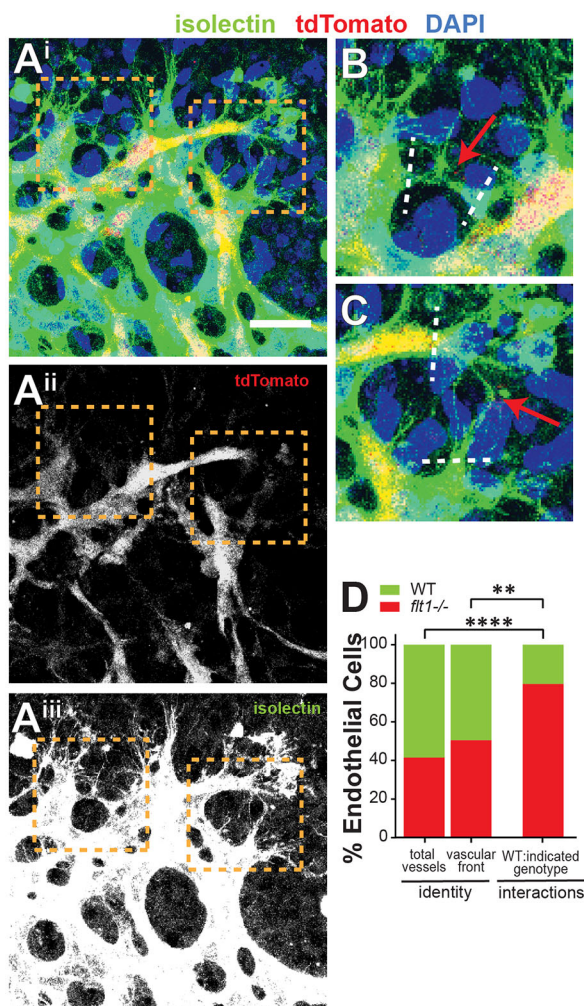
Fig. 1. Flt1 influences retinal vessel interactions *in vivo*. (A) Vascular front of representative mouse P5 retinal vessel with mosaic loss of Flt1. (Ai) Merge visualized with excision reporter (Aii, red), vessels (Aiii, green) and nuclei (blue). Scale bar: 25 µm. (B,C) Higher magnification of left (B) and right (C) boxed regions in A. Arrow, scored interaction; white dotted lines, the area behind the extension used to define the category. (D) Quantification of the ratio of endothelial cell identities (lanes 1, 2) and wild-type endothelial cell interactions with endothelial cells of the indicated genotype (lane 3). *n*=7 retinas, 45 sprouts. Paired two-tailed Student's *t*-test; **P<0.01, ****P<0.0001.
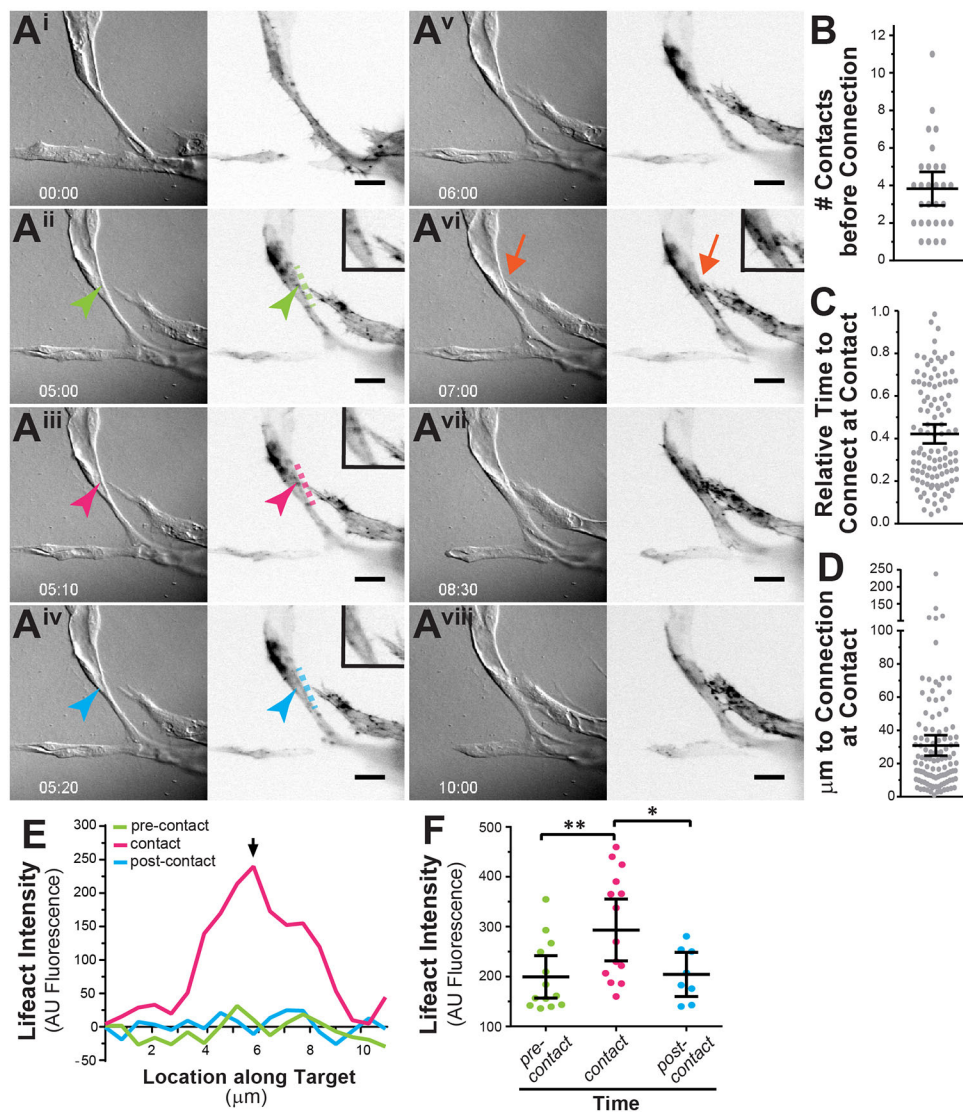
Fig. 2. Blood vessel stable connections are preceded by transient contacts. (A) Live imaging of HUVECs infected with LifeAct. Representative time-lapse stills of DIC (left) and fluorescence (right) channels over d3-5. (Ai-iv) Transient contact. Insets show higher magnification of vessel interaction scan area. Green arrowhead and dotted line, location of pre-contact scan; magenta arrowhead and dotted line, location of transient contact scan; blue arrowhead and dotted line, location of post-contact scan. (Av-viii) Stable connection. Orange arrow, example of stable connection. Time (lower left) is h:min. Scale bars: 25 µm. (B-D) Quantification of transient contact frequency before stable connection (B), and relative time (C) and distance (D) from stable connection site at transient contact. *n*=28 sprouts from 12 movies. (E) Fluorescence intensity of LifeAct at transient contact sites was quantified across the site pre-contact (Aii, green line), at contact (Aiii, magenta line) and post-contact (Aiv, blue line). Arrow indicates position of contact site. (F) Fluorescence intensity of LifeAct at transient contact sites was quantified pre-contact time (example, green arrowhead in Aii), at contact time (example, magenta arrowhead in Aiii) and post-contact time (example, blue arrowhead in Aiv). *n*=14 contacts from 9 movies. One-way ANOVA with Bonferroni's post-hoc correction; *$P<0.05$, **$P<0.01$. Error bars, mean± 95% CI.

of *FLT1* KD on overall morphogenesis. We also generated and validated an siRNA targeting both FLT1 isoforms, and showed that FLT1 reduction increased the phosphoFLK1/total FLK1 ratio in HUVECs, consistent with our hypothesis that *FLT1* manipulations affect vessel anastomosis and morphogenesis via elevated VEGFA signaling (Fig. S2H).

We next focused on how FLT1 levels affected sprout anastomosis. We previously reported that mouse embryonic stem cell (ESC)-derived vessels lacking *Flt1* via genetic deletion connected more frequently, and we attributed this overall increase to a combined increased frequency of sprout initiations and decreased frequency of sprout retractions (Chappell et al., 2016). Here, we used time-lapse imaging to specifically focus on the effects of FLT1 on dynamic aspects of the anastomosis process in sprouting HUVECs (Fig. 3A,B, Movies 2 and 3). Both control and *FLT1* KD sprouts had transient contacts and formed stable connections, but dynamics were altered with reduced FLT1 levels. Connections from *FLT1* KD sprouts formed earlier in the time sequence than those from controls, as measured from the emergence of a 'tip cell' phenotype (cell protrusions and directed migration away from parent vessel) to stable connection, although the overall distance traveled to the target was unaltered (Fig. 3C,D). Consistent with the LifeAct analysis, control sprouts made about four transient contacts prior to forming a

stable connection, but *FLT1* KD sprouts averaged fewer than two transient contacts before forming a stable connection (Fig. 3E).

We also analyzed sprout behavior in ESC-derived vessels that differentiate over a week and form interconnected lumenized blood vessel networks (Rylova et al., 2008). ESCs transgenic for PECAM-eGFP and genetically deleted for *Flt1* (Chappell et al., 2009) also showed earlier connection times, similar connection distances, and reduced numbers of transient contacts prior to stable connection, relative to WT controls (Fig. 3F-J, Movies 4 and 5). These results are consistent with our more global analysis of sprouting morphogenesis in this model (Chappell et al., 2016), as the reduced number of transient contacts and time to connection documented here predict an overall higher connection frequency.

Taken together, these data suggest that sprout anastomosis is a regulated process, and that the number of transient contacts, which may reflect exploratory behavior to gather information about potential targets, is reduced when Flt1 levels are reduced or absent.

Differential FLT1 isoform requirements for sprout anastomosis

Flt1 regulates angiogenesis through both a membrane-bound decoy receptor (mFlt1) and a secreted isoform (sFlt1) that also acts as a ligand sink (Kendall and Thomas, 1993; Roberts et al., 2004). Both
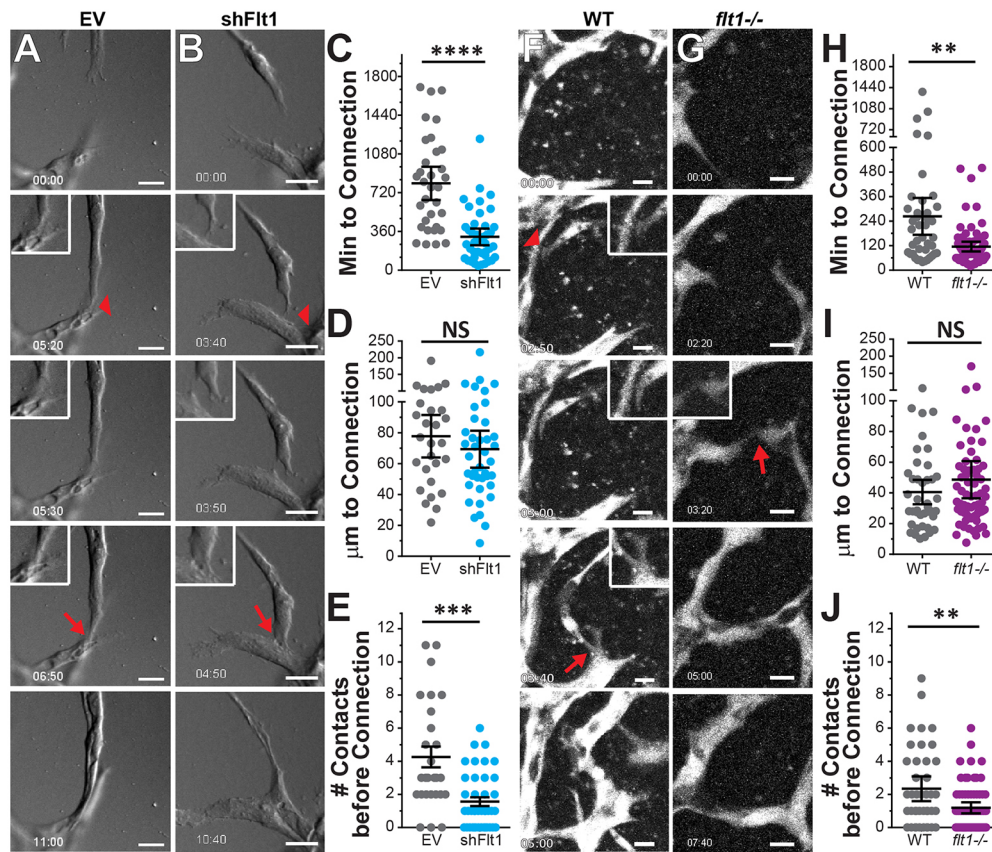
Fig. 3. Transient contact dynamics during vessel anastomosis are regulated by Flt1. (A,B) Representative time-lapse stills of d3-5 HUVEC sprouts infected with lentivirus encoding (EV) control (A) and shFlt1 (B). Transient contact, red arrowhead; stable connection, red arrow. Insets show higher magnification of vessel interactions. Time, h:min. EV control, *n*=27 sprouts; shFlt1, *n*=41 sprouts. (C-E) Quantification of time and distance to connection and the number of contacts made before stable connection for experiments illustrated in A,B. (F,G) Representative time-lapse stills of WT (F) and *Flt1*^{−/−} (G) ESC-derived vessels at d6 of differentiation. Transient contact, red arrowhead; stable connection, red arrow. Insets show higher magnification of vessel interactions. (H-J) Quantification of time and distance to connection and the number of contacts made before stable connection for experiments illustrated in F,G. WT, *n*=88 sprouts; *Flt1*^{−/−}, *n*=48 sprouts. Two-tailed Student's *t*-test; **P<0.01, ***P<001, ****P<0.0001; NS, not significant. Error bars, mean ±95% CI. Scale bars: 25 μm in A,B; 10 μm in F,G.

isoforms can negatively modulate signaling through VEGFA/Flk1 (Kappas et al., 2008; Kendall and Thomas, 1993), but they are predicted to differentiate with regard to cell autonomy, with mFlt1 presumably acting in a cell-autonomous manner, whereas sFlt1 can act non-cell-autonomously because it is secreted. We hypothesized that both activities influence dynamic aspects of anastomosis. We generated isoform-specific siRNAs that selectively reduced the levels of mFLT1 in cell lysates or sFLT1 in conditioned medium (i.e. secreted sFLT1), and validated their efficacy in western blots and the sprouting assay (Fig. 4A-C, Fig. S3A-F). HUVEC sprouts with KD of total FLT1 via siRNA mimicked the effects of the shRNA KD, with no effect on sprouting but significantly increased branching (Fig. S3A,B,E,F). Likewise, selective KD of either isoform did not affect sprouting, but KD of mFLT1 increased branching whereas KD of sFLT1 did not affect branching in this assay, perhaps because the surrounding 3D matrix is somewhat artificial (Fig. S3C-F). We then used live imaging to determine the number of transient contacts that occurred before stable connections formed, and found that KD of either FLT1 isoform reduced the number of transient contacts prior to stable connection (Fig. 4D-G). These results suggest that both FLT1 isoforms are important in regulating the exploratory behavior of sprouts as they approach potential connection targets.

We next examined target sites for transient contacts and stable connections, and asked whether target areas had unique attributes prior to contact or connection. We focused on targets that were part of established vessels or sprouts, as opposed to targets that were other tip cells, so that the incoming (i.e. non-target) sprout in principle had a choice of sites for the formation of transient contacts or stable connections. Live imaging of LifeAct-infected HUVECs in the sprouting angiogenesis assay revealed that some endothelial

cells in the target area exhibited protrusive activity, whereas others were non-protrusive or static (Fig. 5A,B). Analysis of time stamps just prior to transient contact or stable connection showed that subsequent transient contact sites were equally likely to be protrusive or static, consistent with these contacts being largely 'exploratory' in nature. By contrast, sites for stable connection were more likely to exhibit protrusive activity prior to connection (Fig. 5C). Thus, differential cell behavior prior to stable connection correlates with target sites for forming these connections, suggesting that protrusive activity contributes to the spatial selectivity for connection target sites during anastomosis.

Because protrusive activity is associated with endothelial cells that will subsequently form stable connections, and protrusive activity is associated with loss of Flt1 (Chappell et al., 2016), we hypothesized that FLT1 levels within individual target endothelial cells would affect the probability of forming a stable connection. We first examined FLT1 expression at target sites. Endogenous Flt1 levels are heterogeneous in developing blood vessels (Kappas et al., 2008; Chappell et al., 2009), so we predicted that this heterogeneous expression would contribute to target site selection during sprout anastomosis. Fixed-image staining, using PECAM1 to define cell borders and interactions, revealed that FLT1 intensity was decreased in target endothelial cells that were 'touched' by sprouts (note that contacts versus connections cannot be distinguished in the absence of live imaging) compared with neighboring cells (Fig. 5D,E).

Next, we manipulated *FLT1* expression at the target site by generating mosaic HUVEC vessels that were a 50:50 mixture of endothelial cells with *FLT1* KD (green) and control endothelial cells (magenta). The mosaic beads were incubated with control beads coated with unmanipulated endothelial cells lacking reporter expression (Fig. S4A). We then live-imaged unmanipulated

DEVELOPMENT
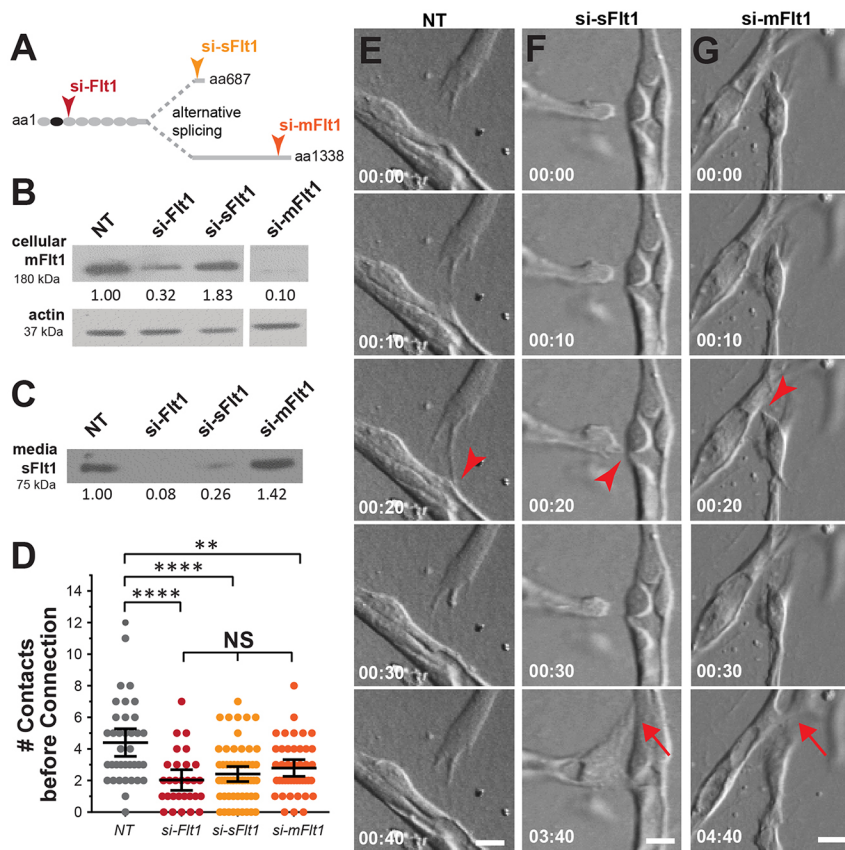
Fig. 4. Both Flt1 isoforms reduce transient contacts prior to connection. (A) Schematic showing Flt1 isoforms and sequences targeted by the indicated siRNAs. (B,C) Western blot of HUVEC lysates (B) and concentrated conditioned media (C) with indicated knockdowns. Control (NT), total *FLT1* KD (si-Flt1), soluble *FLT1* KD (si-sFlt1), membrane-tethered *FLT1* KD (si-mFlt1). Fold change from control is shown beneath lanes. (D) Quantification of the number of contacts prior to connection. One-way ANOVA with Bonferroni's post-hoc correction; **$P<0.01$, ****$P<0.0001$; NS, not significant. Error bars, mean±95% CI. (E-G) Stills from DIC movies showing examples of transient contacts (E-G, red arrowheads) and stable connections (F,G, red arrows) with the indicated treatments. Time, h:min. Scale bars: 10 µm.

sprouts as they approached mosaic target areas to analyze their behavior. Controls in which neither reporter was linked to *FLT1* KD showed no bias in either transient contact or stable connection target site selection, relative to input or to each other (Fig. S4B). By contrast, in experiments in which both control and *FLT1* KD endothelial cells were available as targets, there was a significant bias towards *FLT1* KD endothelial cells as connection targets relative to contact (Fig. 5F, Fig. S4C, Movie 6). These data show that contact and connection biases differ, further supporting our model whereby transient contacts are unbiased exploratory behavior whereas stable connections are biased for target site. These results also show a role for FLT1 in target site selection, indicating that aspects of sprout anastomosis are regulated.

We next examined the role of each FLT1 isoform in the preference for endothelial cells with reduced FLT1 as stable connection sites. We live-imaged mosaic target vessels with control endothelial cells mixed with endothelial cells with KD of total *FLT1*, *mFLT1* or *sFLT1* via siRNA. Similar to total *FLT1* KD by shRNA, siRNA *FLT1* KD endothelial cells were significantly more likely to form stable connections relative to transient contacts, and this bias was recapitulated by selective reduction of mFLT1 from endothelial cells, but not by selective reduction of sFLT1 (Fig. 5G-I). Taken together, these findings indicate that sprouts sample potential targets in an unbiased way via transient contacts, and form stable connections with target site selectivity influenced by relative mFLT1 levels.

DISCUSSION

Here, we highlight dynamic features of blood vessel sprout anastomosis, and find that connection site selection is a regulated rather than completely stochastic process. We show that, in developing vessel networks, connection target site selectivity is

regulated by levels of the VEGF receptor Flt1. We find that numerous transient contacts occur prior to the formation of stable connections. Flt1 regulates the number of transient contacts, but these contacts are unbiased relative to Flt1 levels at individual sites of contact, suggesting that transient contacts are 'exploratory' in nature. By contrast, sites of anastomosis are biased for target endothelial cells with lower levels of Flt1, and presumably higher levels of VEGF signaling (Fig. 5J). This bias depends on mFlt1 but not sFlt1, consistent with the idea that target site selection is regulated in a cell-autonomous manner by a membrane-localized decoy receptor for VEGFA.

The ability of sprouts to transiently contact potential targets prior to, and distinct from, the formation of stable contacts has not been reported in sprouting vessels; instead, previous studies suggest that most interactions between sprouts and vessels result in a stable connection (Lenard et al., 2013; Phng et al., 2013; Gebala et al., 2016). Our results indicate that endothelial cell 'sampling' occurs prior to the formation of stable connections in expanding vessel networks where sprouts have 'choices'. These brief interactions are likely to impart information to the sprout regarding the appropriateness of a given endothelial cell for stable connection. The transient contacts are initiated by cytoplasmic projections from actively migrating sprout tips that include, but are not limited to, filopodia, and have an actin cytoskeleton as revealed by LifeAct labeling. Although we cannot rigorously determine the nature of the actin filaments, we believe the extensions are likely to come from the cortical pool, as there is little evidence of actin-based stress fibers in the motile endothelial tip cells.

We propose that connections formed without the spatial input conferred by heterogeneous Flt1 expression in the target area are more likely to collapse into other vessels in crowded conditions, such as those seen in the ESC-derived vessels, while in the artificial
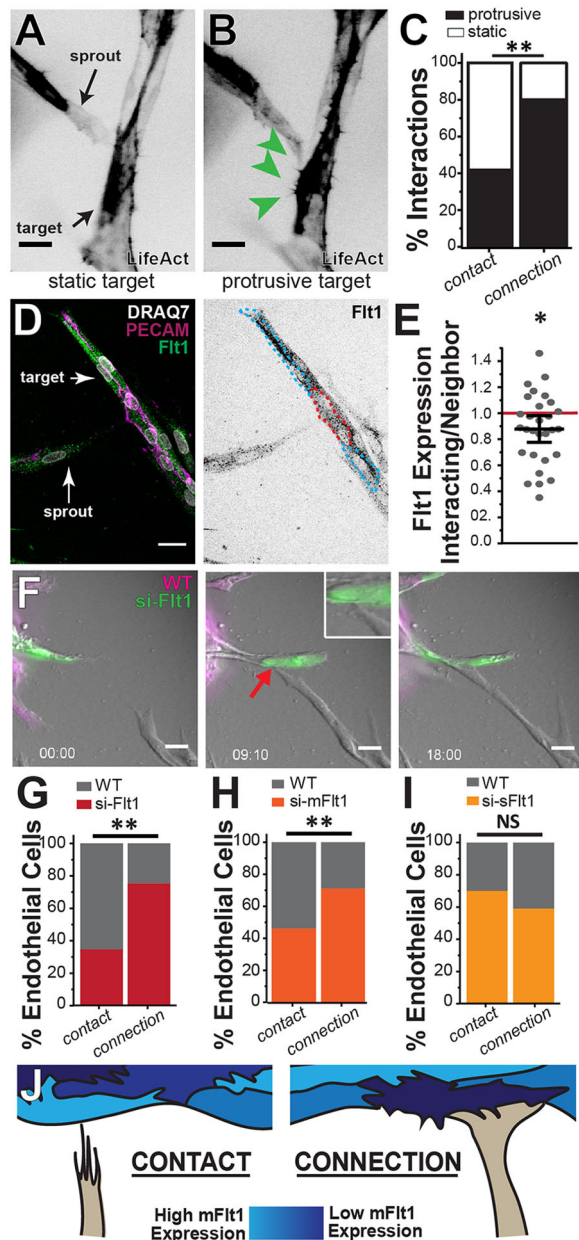
Fig. 5. Target vessel connection site is biased by Flt1. (A,B) Representative images of LifeAct-infected 3D HUVEC sprouts and targets showing transient contacts interacting with a static (A) or protrusive (B) target cell. Green arrowheads, LifeAct-positive protrusions. (C) Quantification of target cell protrusions (see Materials and Methods for definition of 'static' and 'protrusive') at time stamp immediately preceding contact (*n*=63 events) or connection (*n*=18 events). Observed versus expected binomial test; **$P<0.01$. (D) Representative HUVEC vessel at d5 (left; with indicated staining) and Flt1 channel only (right). Interacting target cell (red outline) and neighboring potential target cells (blue outline) of representative HUVEC vessels are noted. (E) The relative Flt1 staining intensity between pairs of endothelial cells was quantified (*n*=29 pairs). Unpaired Student's *t*-test versus no difference (red line); *$P<0.05$. (F) Representative time-lapse images from d3-5 of WT sprout (no label) and target vessel with 50% Flt1 KD endothelial cells (green) and 50% WT cells (magenta). Time, h:min. Stable connection, red arrow. (G-I) Percentage of transient contacts and stable connections with endothelial cells of the indicated type in mosaic target vessels. si-Flt1, *n*=41 contacts from *n*=12 connections; si-mFlt1, *n*=57 contacts from *n*=17 connections; si-sFlt1, *n*=53 contacts from *n*=17 connections. Observed versus expected binomial test; **$P<0.01$; NS, not significant. (J) Schematic of anastomosis dynamics and connection site selection during angiogenesis. Scale bars: 10 µm in A,B; 25 µm in D,F.

matrix the same loss of selectivity increases the overall number of new connections that are scored as branch points in the fixed-image analyses. This idea is supported by our previous finding that connections formed by ESC-derived vessels lacking *Flt1* are less likely to lead to stable connections; instead, these vessels did often collapse into the vessel network without contributing a new conduit (Chappell et al., 2016). Although numerous aspects of Flt1 loss may contribute to this outcome, here we show that sprouts with reduced Flt1 have fewer transient contacts prior to connection, indicating reduced exploratory or sampling behavior that may lead to suboptimal connections in terms of proximity to another connected sprout or vessel. Thus, transient contacts might be a mechanism whereby endothelial sprouts sense the local environment for a connection site optimized to form a new conduit.

Initial analysis of mosaic retinal vessels revealed that WT sprouts interacted more often with *Flt1*$^{-/-}$ cells. This bias was also found in HUVEC mosaic vessel targets with reduced FLT1. Thus, cells with reduced Flt1, which are likely to have higher levels of VEGF signaling, are favored as sites of stable connection, and this bias depends on the expression of the membrane-bound decoy VEGF receptor, mFlt1. Heterogeneous Flt1 expression and Flk1 activity influence sprout initiation and extension (Chappell et al., 2009; Arima et al., 2011; Jakobsson et al., 2010; Kappas et al., 2008; Chappell et al., 2013), and our data extend the regulatory impact of heterogeneous VEGF signaling in the patterning of blood vessels to anastomosis. Membrane-bound Flt1 appears essential for the anastomosis selectivity, which is consistent with its cell-autonomous role in endothelial cells, relative to sFlt1 that is secreted and has potential to affect aspects of sprouting non-cell-autonomously (Chappell et al., 2009; Kappas et al., 2008). Flt1 is required for normal developmental angiogenesis, although not as a signaling receptor (Fong et al., 1995; Hiratsuka et al., 1998), so it is likely that mFlt1 influences connection site selectivity in its role as a membrane-tethered decoy receptor that alters VEGF signaling in endothelial cells (Meyer et al., 2006; Anisimov et al., 2013). Here, we confirm that reduced Flt1 in endothelial cells leads to increased levels of active Flk1 (Kappas et al., 2008; Roberts et al., 2004), which is consistent with our observation of increased protrusive activity of target endothelial cells that appear favored as stable connection sites.

In summary, this work shows that endothelial sprout anastomosis is a regulated process and implicates VEGF signaling in both the exploratory behavior that precedes the formation of stable connections and connection target site choice. These findings suggest that the location and timing of establishing a stable connection are essential in forming a new conduit in vascular beds that do not have an imposed pre-pattern. This requirement for Flt1 in the regulated patterning of anastomoses suggests a novel role for the VEGF signaling pathway in blood vessel patterning, and potentially new ways to regulate vascular network formation with implications for regenerative medicine.

MATERIALS AND METHODS
Retinal angiogenesis imaging and analysis
Mice (*Mus musculus*) with *Flt1*$^{flox/flox}$ alleles (Genentech) were bred with *Tg(UBC-cre/ERT2)* (Jackson Laboratory #007001) mice that also carried the Cre-mediated recombination reporter gene *R26R TdTomato* [*Gt(ROSA) 26Sor*$^{tm14(CAG-tdTomato)Hze}$, Jackson Laboratory #007914]. Mice were maintained in accordance with the University of North Carolina, Chapel Hill, Institutional Animal Care and Use Committee. Mosaic Cre excision of vessels was accomplished by intraperitoneal injection of 0.5 mg/ml tamoxifen (MP Biomedicals) at P2. P5 retinas were perfusion fixed with 0.5% paraformaldehyde (PFA) in PBS, harvested, and fixed for 2 h with 2%

PFA. Retinas were rinsed, stained for isolectin B4 and with DAPI, and mounted using established protocols (Chappell et al., 2009). Images were acquired on a Leica DMI 6000B or Zeiss LSM 880 confocal microscope at 40× magnification, with optimal z-stacks compressed post-acquisition using ImageJ software. Antibodies are detailed in Table S1.

Sprouts were identified at the angiogenic front using previously established methods (Chappell et al., 2009). Cellular genetic identity was classified from reporter expression during analysis, and interactions between sprouts and other sprouts/vessels were identified as overlap of cellular extensions with other extensions/cells in the isolectin B4 channel. Excision within retinal vessels was scored by comparing the percentage of isolectin$^+$/tdTomato$^-$/DAPI$^+$ endothelial cells (wild-type) with isolectin$^+$/tdTomato$^+$/DAPI$^+$ ($Flt1^{-/-}$) endothelial cells in the indicated areas of the retinal vasculature at P5.

Cell lines and culture

HUVECs (Lonza) were maintained in EBM-2 media with the EGM Bullet Kit and 1× antibiotic/antimycotic (Sigma) according to the manufacturer's directions. Normal human lung fibroblasts (Lonza) were maintained in high-glucose DMEM supplemented with 10% FBS and 1× antibiotic/antimycotic. ESCs isolated from WT mice and $Flt1^{-/-}$ mice (gift from G.H. Fong) were maintained and differentiated as previously described (Rylova et al., 2008).

Protein quantification

Protein analysis was performed on culture medium after concentration using Pierce Protein Concentrators (10 MWCO, Fisher Scientific) or on cell lysates collected in radioimmunoprecipitation assay buffer plus 1×protease inhibitor cocktail (Cell Signaling). Western blot analysis was performed 48 h after lentivirus infection or siRNA transfection. Briefly, protein was quantified by the Bradford reaction (Bio-Rad) and equivalent protein amounts were subject to 7.5% SDS-PAGE. Protein was transferred to a polyvinylidene fluoride membrane, stained with Ponceau S solution to visualize transferred protein and then incubated with the appropriate primary antibody in Tris-buffered saline (TBS) or PBS with 0.5% Triton X-100 (Sigma). Horseradish peroxidase-conjugated secondary antibody was incubated with membranes for 1 h at room temperature and chemiluminescent detection was performed using Luminata Forte Western Substrate (EMD Millipore). Antibodies are detailed in Table S1.

Lentivirus and siRNA knockdown

The Flt1 shRNA construct (RHS3979-201732907, Dharmacon) was modified to include GFP in addition to shFlt1. Lentivirus was produced by the UNC LentiCore Facility. Lentivirus was incubated with endothelial cells for 6 h with addition of 0.25 µg/ml polybrene (EMD Millipore). Lentiviral infection with LifeAct-GFP or LifeAct-RFP [gift from Rusty Lansford (Addgene plasmid #51010) or Weiping Han (Addgene plasmid #64048), respectively] allowed for visualization of F-actin.

siRNA KD was performed by 6 h incubation with RNAimax (Invitrogen) and a commercially designed and validated targeted construct against total Flt1 (Life Technologies) or siRNA constructs, self-designed and self-validated with locked nucleic acid (LNA) ends, targeting the unique portions of either sFlt1 or mFlt1 (Exiqon). Targeted sequences are listed in Table S2. KD by shRNA infection was initially assessed by qRT-PCR (see Table S3 for primers) and western blot and confirmed by GFP fluorescence; subsequent shRNA KD efficiency was assessed by GFP fluorescence. Transfection efficiency for isoform-selective KD was quantified by western blot for each experiment.

HUVEC sprouting angiogenesis assay imaging and analysis

The HUVEC sprouting angiogenesis assay was set up as described (Nakatsu and Hughes, 2008). Briefly, HUVECs were trypsinized, combined with Cytodex microcarrier beads (Sigma), then incubated with periodic agitation for 4 h. Following overnight growth, the HUVEC-coated microcarrier beads were embedded in a 1.5% fibrinogen-thrombin gel that was allowed to polymerize at 37°C for 15-45 min, and then a layer of normal lung fibroblasts was seeded on top of the solidified fibrinogen gel.

Dynamic imaging of d3-5 HUVEC sprouts and vessels was performed on an Olympus VivaView incubator fluorescence inverted microscope at 10× magnification with image acquisition at 10 min intervals for 42 h. Fixed imaging was performed at d5. After removing fibroblasts, cultures were fixed with 4% PFA for 15 min at room temperature. Cultures were permeabilized using 0.1% Triton X-100 (Sigma) in TBS or PBS for 2-4 h at room temperature and then blocked at 4°C overnight in TBS or PBS with 0.1% Tween 20 (TBST or PBST) and 5% goat serum (blocking buffer). Primary antibodies were incubated as indicated in Table S1, washed with blocking buffer overnight and incubated overnight at 4°C with either goat anti-mouse Alexa-Fluor-conjugated secondary or goat anti-rabbit Alexa-Fluor-conjugated secondary in TBST or PBST (Life Technologies). Confocal images were acquired on an Olympus FV1200 system using a 10× objective (NA 0.40) and optimal z-stacks, compressed post-acquisition for analysis.

Vessel interactions were scored when two cell bodies overlapped in either the DIC or fluorescent channels, depending upon the experimental setup. Interactions classified as transient contacts were defined as overlap in a single time frame, therefore lasting less than 10 min. Stable connections were defined as overlap that persisted for at least three time frames, therefore lasting a minimum of 20 min. Target vessel activity was classified as static or protrusive based upon the endothelial cells within 30 µm of the interaction site. Static vessels exhibited no LifeAct-labeled protrusions extending away from the vessel axis, while protrusive vessels contained a minimum of three extensions, defined as fluorescent protrusions >4 µm. LifeAct intensity was determined by performing a line scan (e.g. Fig. 2A) and subtracting nearby background in the time frame of the contact from the raw values. Maximum intensity of the line scan at three time frames was used to calculate intensity/time.

ESC-derived vessel imaging and analysis

Generation of ESC lines expressing PECAM-eGFP was previously reported (Kearney et al., 2004). Dynamic imaging of d7-8 differentiating ESC cultures was performed as follows: confocal images at either 10× or 20× magnification using an Olympus FluoView FV1000 or FV10i system, both with full environmental chambers, were acquired at 4-10 min intervals for 16-20 h. A z-stack, with 4-6 µm between focal planes, of 6-8 images was acquired at each time point. Post-acquisition compression of z-stack images into a single image was performed for each time point.

Fluorescence-activated cell sorting (FACS) analysis

HUVECs were sorted by FACS as described in supplementary Materials and Methods.

mRNA preparation and quantification

RNA was collected 48 h post-treatment, converted to cDNA and analyzed by qRT-PCR as described in supplementary Materials and Methods.

Statistical analysis

Statistical analyses were performed using GraphPad Prism 6 software. $P<0.05$ was considered statistically significant. Statistical methods and significance are noted in the figure legends.

Competing interests
The authors declare no competing or financial interests.

Author contributions
J.E.N. designed and performed experiments, interpreted and analyzed results, and wrote the manuscript. J.C.C. performed some experiments and analysis. J.G.C. performed some analysis. V.L.B. conceptualized experiments, interpreted results and wrote and edited the manuscript.

Supplementary information
Supplementary information available online at
http://dev.biologists.org/lookup/doi/10.1242/dev.145672.supplemental

References

Adams, R. H. and Alitalo, K. (2007). Molecular regulation of angiogenesis and lymphangiogenesis. *Nat. Rev. Mol. Cell Biol.* **8**, 464-478.

Anisimov, A., Leppänen, V.-M., Tvorogov, D., Zarkada, G., Jeltsch, M., Holopainen, T., Kaijalainen, S. and Alitalo, K. (2013). The basis for the distinct biological activities of vascular endothelial growth factor receptor-1 ligands. *Sci. Signal.* **6**, ra52.

Arima, S., Nishiyama, K., Ko, T., Arima, Y., Hakozaki, Y., Sugihara, K., Koseki, H., Uchijima, Y., Kurihara, Y. and Kurihara, H. (2011). Angiogenic morphogenesis driven by dynamic and heterogeneous collective endothelial cell movement. *Development* **138**, 4763-4776.

Betz, C., Lenard, A., Belting, H.-G. and Affolter, M. (2016). Cell behaviors and dynamics during angiogenesis. *Development* **143**, 2249-2260.

Blanco, R. and Gerhardt, H. (2013). VEGF and Notch in tip and stalk cell selection. *Cold Spring Harb. Perspect. Med.* **3**, a006569.

Carmeliet, P. (2005). Angiogenesis in life, disease and medicine. *Nat. Cell Biol.* **438**, 932-936.

Chappell, J. C. and Bautch, V. L. (2010). Vascular development—genetic mechanisms and links to vascular disease. *Curr. Top. Dev. Biol.* **90**, 43-72.

Chappell, J. C., Taylor, S. M., Ferrara, N. and Bautch, V. L. (2009). Local guidance of emerging vessel sprouts requires soluble Flt-1. *Dev. Cell* **17**, 377-386.

Chappell, J. C., Wiley, D. M. and Bautch, V. L. (2011). Regulation of blood vessel sprouting. *Semin. Cell Dev. Biol.* **22**, 1005-1011.

Chappell, J. C., Mouillesseaux, K. P. and Bautch, V. L. (2013). Flt-1 (vascular endothelial growth factor receptor-1) is essential for the vascular endothelial growth factor–notch feedback loop during angiogenesis. *Arterioscler. Thromb. Vasc. Biol.* **33**, 1952-1959.

Chappell, J. C., Cluceru, J. G., Nesmith, J. E., Mouillesseaux, K. P., Bardley, V. B., Hartland, C. M., Hashambhoy-Ramsay, Y. L., Walpole, J., Peirce, S. M., Mac Gabhann, F. et al. (2016). Flt-1 (VEGFR-1) coordinates discrete stages of blood vessel formation. *Cardiovasc. Res.* **111**, 84-93.

Drake, C. J. and Fleming, P. A. (2000). Vasculogenesis in the day 6.5 to 9.5 mouse embryo. *Blood* **95**, 1671-1679.

Fong, G.-H., Rossant, J., Gertsenstein, M. and Breitman, M. L. (1995). Role of the Flt-1 receptor tyrosine kinase in regulating the assembly of vascular endothelium. *Nature* **376**, 66-70.

Gebala, V., Collins, R., Geudens, I., Phng, L.-K. and Gerhardt, H. (2016). Blood flow drives lumen formation by inverse membrane blebbing during angiogenesis in vivo. *Nat. Cell Biol.* **18**, 443-450.

Geudens, I. and Gerhardt, H. (2011). Coordinating cell behaviour during blood vessel formation. *Development* **138**, 4569-4583.

Hanahan, D. and Weinberg, R. A. (2011). Hallmarks of cancer: the next generation. *Cell* **144**, 646-674.

Hiratsuka, S., Minowa, O., Kuno, J., Noda, T. and Shibuya, M. (1998). Flt-1 lacking the tyrosine kinase domain is sufficient for normal development and angiogenesis in mice. *Proc. Natl. Acad. Sci. USA* **95**, 9349-9354.

Ho, V. C., Duan, L.-J., Cronin, C., Liang, B. T. and Fong, G.-H. (2012). Elevated vascular endothelial growth factor receptor-2 abundance contributes to increased angiogenesis in vascular endothelial growth factor receptor-1-deficient mice. *Circulation* **126**, 741-752.

Ito, N., Wernstedt, C., Engström, U. and Claesson-Welsh, L. (1998). Identification of vascular endothelial growth factor receptor-1 tyrosine phosphorylation sites and binding of SH2 domain-containing molecules. *J. Biol. Chem.* **273**, 23410-23418.

Jakobsson, L. Franco, C. A., Bentley, K., Collins, R. T., Ponsioen, B., Aspalter, I. M., Rosewell, I., Busse, M., Thurston, G., Medvinsky, A. et al. (2010). Endothelial cells dynamically compete for the tip cell position during angiogenic sprouting. *Nat. Cell Biol.* **12**, 943-953.

Kappas, N. C., Zeng, G., Chappell, J. C., Kearney, J. B., Hazarika, S., Kallianos, K. G., Patterson, C., Annex, B. H. and Bautch, V. L. (2008). The Notch ligand Delta-like 4 negatively regulates endothelial tip cell formation and vessel branching. *J. Cell Biol.* **181**, 3225-3230.

Kappas, N. C., Zeng, G., Chappell, J. C., Kearney, J. B., Hazarika, S., Kallianos, K. G., Patterson, C., Annex, B. H. and Bautch, V. L. (2008). The VEGF receptor Flt-1 spatially modulates Flk-1 signaling and blood vessel branching. *J. Cell Biol.* **181**, 847-858.

Kearney, J. B., Kappas, N. C., Ellerstrom, C., DiPaola, F. W. and Bautch, V. L. (2004). The VEGF receptor flt-1 (VEGFR-1) is a positive modulator of vascular sprout formation and branching morphogenesis. *Blood* **103**, 4527-4535.

Kendall, R. L. and Thomas, K. A. (1993). Inhibition of vascular endothelial cell growth factor activity by an endogenously encoded soluble receptor. *Proc. Natl. Acad. Sci. USA* **90**, 10705-10709.

Khurana, R., Simons, M., Martin, J. F. and Zachary, I. C. (2005). Role of angiogenesis in cardiovascular disease: a critical appraisal. *Circulation* **112**, 1813-1824.

Koch, S., Tugues, A., Li, X., Gualandi, L. and Claesson-Welsh, L. (2011). Signal transduction by vascular endothelial growth factor receptors. *Biochem. J.* **437**, 169-183.

Larrivée, B., Frieta, C., Suchting, S., Brunet, I. and Eichmann, A. (2009). Guidance of vascular development: lessons from the nervous system. *Circ. Res.* **104**, 428-441.

Lenard, A., Ellertsdottir, E., Herwig, L., Krudewig, A., Sauteur, L., Belting, H.-G. and Affolter, M. (2013). In vivo analysis reveals a highly stereotypic morphogenetic pathway of vascular anastomosis. *Dev. Cell* **25**, 492-506.

Meyer, R. D., Mohammadi, M. and Rahimi, N. (2006). A single amino acid substitution in the activation loop defines the decoy characteristic of VEGFR-1/ FLT-1. *J. Biol. Chem.* **281**, 867-875.

Nakatsu, M. N. and Hughes, C. C. W. (2008). An optimized three-dimensional in vitro model for the analysis of angiogenesis. *Methods Enzymol.* **443**, 65-82.

Phng, L.-K., Stanchi, F. and Gerhardt, H. (2013). Filopodia are dispensable for endothelial tip cell guidance. *Development* **140**, 4031-4040.

Risau, W. and Flamme, I. (1995). Vasculogenesis. *Annu. Rev. Cell Dev. Biol.* **11**, 73-91.

Roberts, D. M., Kearney, J. B., Johnson, J. H., Rosenberg, M. P., Kumar, R. and Bautch, V. L. (2004). The vascular endothelial growth factor (VEGF) receptor Flt-1 (VEGFR-1) modulates Flk-1 (VEGFR-2) signaling during blood vessel formation. *Am. J. Pathol.* **164**, 1531-1535.

Rylova, S. N., Randhawa, P. K. and Bautch, V. L. (2008). In vitro differentiation of mouse embryonic stem cells into primitive blood vessels. *Methods Enzymol.* **443**, 103-117.

Shibuya, M. (2013). Vascular endothelial growth factor and its receptor system: physiological functions in angiogenesis and pathological roles in various diseases. *J. Biochem.* **153**, 13-19.

Simons, M., Gordon, E. and Claesson-Welsh, L. (2016). Mechanisms and regulation of endothelial VEGF receptor signalling. *Nature* **17**, 611-625.

Xu, K. and Cleaver, O. (2011). Tubulogenesis during blood vessel formation. *Semin. Cell Dev. Biol.* **22**, 993-1004.

DEVELOPMENT